Raman-Induced Polarization-Dependent Gain in Parametric Amplifiers Pumped With Orthogonally Polarized Lasers

Q. Lin, F. Yaman, and Govind P. Agrawal

***Abstract*—Fiber-optic parametric amplifiers are often pumped using two orthogonally polarized lasers. We show that, contrary to a common belief, such amplifiers exhibit polarization-dependent gain (PDG) because of the contribution of Raman scattering to the underlying four-wave mixing (FWM) process. Such PDG results not only from Raman gain/loss on the signal/idlers imposed by the pumps, but also from variations of FWM efficiency caused by Raman-induced refractive index changes.**

***Index Terms*—Nonlinear optics, optical fibers, optical parametric amplifiers, polarization, Raman scattering.**

FIBER-OPTIC parametric amplifiers (FOPAs), based on four-wave mixing (FWM), occurring inside highly nonlinear fibers (HNLFs) or photonic-crystal fibers, are useful for all-optical ultrafast signal processing. Dual-pump FOPAs are preferred in practice because they provide considerable flexibility through independent control of individual pumps. Polarization-independent operation is essential for practical FOPAs to ensure that the same performance is realized for signals with any input state of polarization (SOP). It is commonly accepted that the nondegenerate FWM process implemented with two orthogonal linearly polarized pumps is intrinsically polarization independent and it can provide a relatively uniform gain over a broad bandwidth [1]–[5]. Polarization-dependent gain (PDG) observed experimentally in such a configuration is attributed to the impact of fiber birefringence [2], [4], [6].

The absence of PDG for orthogonally polarized pumps holds when the underlying FWM results from the instantaneous electronic response. However, the third-order nonlinear response of optical fibers also depends on the retarded molecular response. Because of the latter, the FWM process is inevitably accompanied with Raman scattering [7], [8] that is known to exhibit a strong polarization dependence [9]. In this letter, we develop a vector theory of FWM that includes the Raman contribution and show that the orthogonally polarized pumping configuration exhibits considerable PDG because of a retarded Raman response.

To show the underlying physics as simply as possible, we focus on an isotropic fiber without birefringence. The propagation of optical waves inside such a fiber is described by [8]

$$\frac{\partial \mathbf{A}}{\partial z} = \sum_m i^{m+1} \frac{\beta_m}{m!} \frac{\partial^m \mathbf{A}}{\partial t^m} + i\gamma \mathbf{R}_{\rm NL} \tag{1}$$

Manuscript received June 21, 2005; revised November 7, 2005. This work was supported by the National Science Foundation under Grant ECS-0 320 816 and Grant ECS-0 334 982.

The authors are with the Institute of Optics, University of Rochester, Rochester, NY 14627 USA.

Digital Object Identifier 10.1109/LPT.2005.862365

where β_m is the mth-order dispersion parameter at the carrier frequency ω_0. The nonlinear parameter $\gamma = n_2\omega_0/(ca_{\rm eff})$, where $n_2 \approx 2.6 \times 10^{-20}$ m^2/W for silica fibers and $\alpha_{\rm eff}$ is the effective core area [10]. The Jones vector $\mathbf{A}$ is formed with linearly polarization field components A_x and A_y. The third-order nonlinear response $\mathbf{R}_{\rm NL}(z,t)$ has the general form [8]

$$\begin{aligned}\mathbf{R}_{\rm NL}(z,t) &= (1-f_R)\left\{\frac{2}{3}[\mathbf{A}^*(z,t)\cdot\mathbf{A}(z,t)]\mathbf{A}(z,t) + \frac{1}{3}[\mathbf{A}(z,t)\cdot\mathbf{A}(z,t)]\mathbf{A}^*(z,t)\right\} \\ &\quad + f_R\mathbf{A}(z,t)\int_{-\infty}^{t} dt' h_R(t-t')[\mathbf{A}^*(z,t')\cdot\mathbf{A}(z,t')]\end{aligned} \tag{2}$$

where $h_R(t)$ is the Raman response function, assumed to be isotropic because of a negligible anisotropic part [8], [9], and f_R represents its fractional contribution when h_R is normalized such that $\tilde{H}(0) = 1$, where $\tilde{H}(\Omega)$ is the Fourier transform of $h_R(t)$ defined as $\tilde{H}(\Omega) = \int_{-\infty}^{\infty} h_R(t)\exp(i\Omega t)dt$.

Dual-pump FOPAs operate such that multiple FWM interactions among the four sidebands shown in Fig. 1 occur simultaneously. More specifically, if ω_l and ω_h are frequencies of the two pumps and ω_1 is the signal frequency, three idlers are generated through the frequency combinations $\omega_l + \omega_h \rightarrow \omega_1 + \omega_2, 2\omega_l \rightarrow \omega_1 + \omega_3, 2\omega_h \rightarrow \omega_2 + \omega_4, \omega_l + \omega_2 \rightarrow \omega_h + \omega_3$, and $\omega_h + \omega_1 \rightarrow \omega_l + \omega_4$. In our analysis, we include all six fields but assume that they are in the form of CW waves.

Substituting the total field $\mathbf{A} = \sum_j \mathbf{A}_j e^{-i(\omega_j - \omega_0)t}$ in (1) and decomposing it into different frequency components, we can find the equations governing the evolution of each individual wave $\mathbf{A}_j$ along the fiber. When the two pumps are orthogonally and linearly polarized, they maintain their SOPs along the fiber. We assume that they are polarized along the x and y axes, respectively, and that they remain nearly undepleted. Using $\mathbf{A}_l = A_l\hat{e}_x$ and $\mathbf{A}_h = A_h\hat{e}_y$, pumps satisfy

$$\frac{dA_j}{dz} = ik_jA_j + i\gamma[P_j + (2+f_R)P_s/3]A_j \tag{3}$$

where $k_j = \sum_m \frac{1}{m!}\beta_m(\omega_j - \omega_0)^m$ is the propagation constant at the frequency ω_j and $P_j = |A_j|^2$ is the pump power ($j, s = l, h$ and $j \neq s$). Equation (3) can be easily solved analytically. We find that P_j does not change with z because the Kerr nonlinearity only leads to a nonlinear phase shift through self- and cross-phase modulation. Note that no power transfer

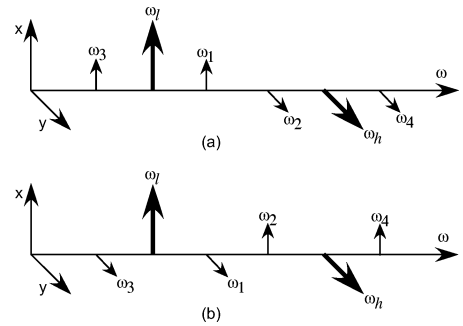

Fig. 1. Illustration of two independent FWM processes for pumping configuration in which two pumps at ω_l and ω_h are linearly polarized along orthogonal x and y axes. Signal at ω_1 produces three distinct idlers at ω_2, ω_3, and ω_4.

occurs between the two orthogonally polarized pumps for an isotropic Raman response.

A detailed analysis shows that various FWM processes can be decoupled into two sets of independent eigen-processes shown in Fig. 1, resulting in the following:

$$\frac{dA_{1x}}{dz} = ik_1A_{1x} + i\gamma\{\eta_{1l}(4)P_lA_{1x} + \eta_{h2}(2)A_lA_hA_{2y}^* + \eta_{l3}(3)A_l^2A_{3x}^* + \eta_{4h}(2)A_lA_h^*A_{4y}\} \quad (4)$$

$$\frac{dA_{1y}}{dz} = ik_1A_{1y} + i\gamma\left\{\eta_{1h}(4)P_hA_{1y} + \eta_{l2}(2)A_lA_hA_{2x}^* + \frac{1}{3}(1-f_R)A_l^2A_{3y}^* + \frac{2}{3}(1-f_R)A_lA_h^*A_{4x}\right\} \quad (5)$$

where η_{js} is denned as $\eta_{js}(m) = m(1-f_R)/3+f_R\tilde{H}(\omega_j-\omega_s)$. To obtain (4) and (5), a common phase factor has been removed from all waves with the transformation $\mathbf{A} \rightarrow \mathbf{A}\exp[-i(2+f_R)\gamma P_0 z/3]$, where $P_0 = P_l + P_h$ is the total pump power. Similar equations for the three idlers can be obtained from (4) and (5) by considering the symmetry among the four sidebands. Equations for the idler at ω_3 are obtained by exchanging subscripts 1 and 2 with 3 and 4, respectively; those for the idler at ω_2 are obtained by exchanging subscripts $l, 1, 3, x$ with $h, 2, 4, y$, respectively; and those for the idler at ω_4 are obtained by exchanging subscripts $l, 1, 2, x$ with $h, 4, 3, y$, respectively.

As the two pump powers are constant along the fiber, the resulting set of linear equations can be easily solved to obtain the parametric gain. Fig. 2 shows examples of the gain spectra for x and y polarized signals using a 500-m-long fiber with its zero-dispersion wavelength (ZDWL) at 1550 nm and an effective area of $\alpha_{\text{eff}} = 10\ \mu\text{m}^2$, corresponding to $\gamma \approx 10.5\ \text{W}^{-1}/\text{km}$. The Raman gain spectrum is obtained from [7] with a peak value of $g \equiv 2n_2\omega_0 f_R\text{Im}[\tilde{H}(\Omega_R)]/c = 0.62 \times 10^{-13}\text{m/W}$ in the 1550-nm regime [9], [11], where $\Omega_R/(2\pi) = 13.2$ THz is the Raman frequency shift and Im denotes the imaginary part. The parametric gain spectra without Raman response ($f_R = 0$) are also presented for comparison with thin solid lines.

When the Raman scattering is absent, the central portion of gain spectra is polarization independent, as expected, since it arises mainly from the polarization-independent FWM process $\omega_l + \omega_h \rightarrow \omega_1 + \omega_2$. The residual polarization dependence near the spectral edges is due to the modulational instability (MI) induced by the two pumps ($2\omega_l \rightarrow \omega_1 + \omega_3$ and $2\omega_h \rightarrow \omega_2 + \omega_4$). For the same reason, MI peaks appear in the vicinity of the pumps. However, parametric gain spectra change in the presence of Raman scattering. The central part of the gain spectrum is no longer uniform even for a fixed signal SOP. When signal is x polarized, FOPA gain increases with increasing signal wavelength, and the opposite occurs when the signal is y polarized. Moreover, the FOPA gain in the central part becomes significantly polarization dependent. Indeed, PDG can be up to 2 dB, depending on the signal wavelength. Such a large PDG has its origin in the polarization dependence of Raman scattering and has consequences for practical applications of FOPAs.

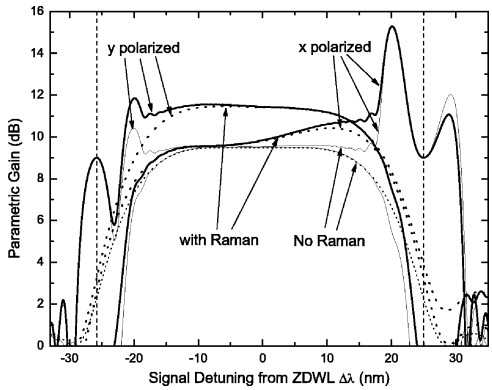

Fig. 2. Parametric gain spectrum for x and y polarized signals as function of signal detuning from ZDWL of fiber located at 1550 nm with $\beta_3 = 0.0378\text{ps}^3/\text{km}$ and $\beta_4 = 1.0 \times 10^{-4}\text{ps}^4/\text{km}$. FOPA is pumped at $\lambda_l = 1575.0$ nm and $\lambda_h = 1524.2$ nm (vertical dashed lines) with equal powers of 0.5 W. Thick and thin curves show cases with and without Raman scattering, respectively. Dotted curves show analytic solution when only single nondegenerate FWM process is considered.

Although a complete description of FOPA based on (4) and (5) is relatively complicated, the central portion of FOPA gain spectrum results mainly from the nondegenerate FWM process $\omega_l + \omega_h \rightarrow \omega_1 + \omega_2$. If only this process is considered, (4) and (5) can be simplified by neglecting the terms containing $\mathbf{A}_3$ and $\mathbf{A}_4$. The resulting simplified equations, together with those for ω_2, can be solved to provide the following analytical solution when only signal at ω_1 is launched at the input [10]:

$$P_{1x}(L) = P_{1\text{x}}(0)\rho_l(L)|\cosh(g_lL) + ik_l\sinh(g_lL)/(2g_l)|^2 \quad (6)$$

$$P_{2x}(L) = \gamma^2|\eta_{1h}(2)|^2P_lP_hP_{1y}(0)\rho_h(L)\,|\sinh(g_hL)|^2/|g_h|^2 \quad (7)$$

where $\kappa_j = k_1 + k_2 - k_l - k_h + \gamma\eta_{1j}(3)P_0 (j = l, h)$ is the total phase mismatch, $g_j^2 = [\gamma\eta_{1j}(2)]^2P_lP_h - (\kappa_j/2)^2$, and $\rho_j(L) = \exp\{\gamma f_R L\Delta_j\text{Im}[\tilde{H}(\omega_1-\omega_j)]\}$, where $\Delta_j = P_h - P_l$ when $j = l$ but $\Delta_j = P_l - P_h$ when $j = h$. The expressions for P_{1y} and P_{2y} can be obtained from (6) and (7) by exchanging the subscript l and x with h and y, respectively. The dotted curves in Fig. 2 show the analytical results. As expected, they agree well with those obtained with the complete four-sideband model over the central portion of gain spectrum.

The physical origin of PDG observed in Fig. 2 can now be easily understood from (6) (where P_{1x} and P_{1y} depend only on $\tilde{H}(\omega_1 - \omega_l)$ and $\tilde{H}(\omega_1 - \omega_h)$, respectively). Raman scattering affects parametric generation in two ways. First, although the Raman response has no impact on orthogonally polarized

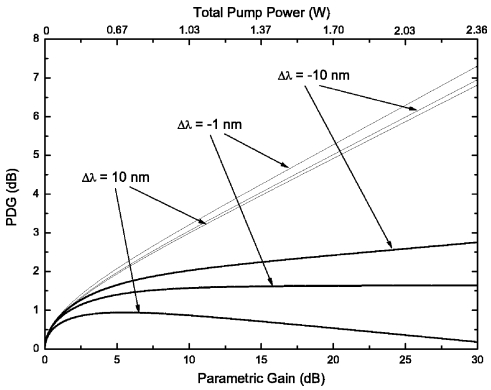

Fig. 3. PDG as function of parametric gain and total pump power at three signal wavelengths under perfect phase-matching condition. Two pumps are assumed to have equal powers $P_l = P_h$. Other conditions are identical to Fig. 2. Parametric gain in horizontal axis is defined as polarization-independent FOPA gain in absence of Raman scattering. Thin curves show comparison PDG induced by pure Raman gain/loss at same signal wavelengths.

waves, it produces gain for the *copolarized* Stokes and loss for the *copolarized* anti-Stokes [determined by $\mathrm{Im}(\tilde{H})$]. In the case of Fig. 1(a), ω_1 experiences Raman loss from the ω_l pump but ω_2 experiences Raman gain from the ω_h one. The situation is reversed in the case of Fig. 1(b), where ω_1 experiences Raman gain from the ω_h pump but ω_2 suffers from Raman loss from the ω_l one. The gain/loss amount depends on the frequency separation between the pumps and signal. Although typical frequency separations in a FOPA are not close to the Raman gain peak, the broad-band nature of the Raman gain spectrum contributes considerable gain/loss to the signal and idlers in the central portion of parametric gain spectrum.

Second, a retarded Raman response changes fiber's refractive index [through $\mathrm{Re}(\tilde{H})$] by an amount that depends on frequency separation between the pumps, signal, and idler. For example, change is about 5% when the signal is detuned from the pump by 30 nm. As the Raman response affects only the *copolarized* waves, variations in the refractive index are determined by the frequency separation $|\omega_1 - \omega_l|$ in the case of Fig. 1(a), but by $|\omega_h - \omega_1|$ in the case of Fig. 1(b). Asymmetry between these two processes produces different FWM efficiencies: It not only induces polarization dependence of parametric generation for a fixed signal frequency but also affects the spectral dependence of parametric gain for a fixed signal SOP. Note that this is quite different from the copolarized pumping configuration in which the signal and idler act simultaneously as the Stokes of one pump and anti-Stokes of the other, resulting in a negligible impact on the refractive index.

Fig. 3 shows PDG as a function of parametric gain obtained from (6), assuming a perfect phase matching $[\mathrm{Re}(\kappa_j) = 0, j = l, h]$. PDG is defined as PDG $\equiv G_y - G_x$, where $G_j = 10\log_{10}[P_{1j}(L)/P_{1j}(0)](j = x, y)$ is the parametric gain for two signal SOPs. The PDG caused by pure Raman gain/loss, defined as $\mathrm{PDG}_R \equiv (10/\ln 10)2\gamma f_R L\{\mathrm{Im}[\tilde{H}(\omega_h - \omega_1)]P_h - \mathrm{Im}[\tilde{H}(\omega_l - \omega_1)]P_l\}$, is also shown by thin curves for comparison. When parametric gain is small, PDG increases with parametric gain and is close to PDG_R. This is because Raman scattering dominates when FWM is negligible, and (6) reduces to $P_{3x}(L) \sim P_{3x}(0)\exp\{2\gamma f_R L P_l \mathrm{Im}[\tilde{H}(\omega_l - \omega_1)]\}$. When parametric gain becomes significant, PDG changes almost linearly with it, but at a smaller rate compared with PDG_R. When $\Delta\lambda = -10$ nm, PDG increases to only 2.7 dB even for a 30-dB gain, much smaller than 7-dB PDG_R. Around the center of parametric gain spectrum ($\Delta\lambda = -1$ nm), PDG is almost constant at 1.6 dB. However, PDG remains small when $\Delta\lambda = 10$ nm and even tends to vanish for large gain. The reason for this behavior is that, when FWM dominates, (6) is approximated by $P_{3x}(L) \sim P_{3x}(0)\exp\{\gamma L\sqrt{P_h P_l}\{4/3 + 2\mathrm{Re}[\tilde{H}(\omega_l - \omega_1)]\}\}$. Raman scattering is suppressed by FWM [12] and PDG is dominated by refractive index changes induced by $\mathrm{Re}(\tilde{H})$, which are smaller than those induced directly by Raman gain/loss. In this case, FWM helps to mitigate the amount of PDG.

In conclusion, we have shown that Raman scattering affects considerably the process of parametric generation inside optical fibers. In contrast to a prevailing belief, the orthogonal-pumping configuration is intrinsically polarization dependent and thus does not provide polarization-independent parametric gain even for isotropic fibers. A retarded Raman response of optical fibers sets a fundamental limit on its polarization dependence. For practical applications of FOPAs, additional techniques may be necessary to reduce such PDG. Furthermore, as the Raman process is rather noisy because of the involvement of thermal phonons, Raman scattering is also expected to affect the noise properties of FOPAs. In particular, it would increase the noise figure of FOPAs and make it polarization dependent because of the asymmetry of Raman contribution to the two eigen processes in Fig. 1. This issue is beyond the scope of this letter and will be discussed elsewhere.

REFERENCES

[1] K. K. Y. Wong, M. E. Marhic, K. Uesaka, and L. G. Kazovsky, "Polarization-independent two-pump fiber optical parametric amplifier," *IEEE Photon. Technol. Lett.*, vol. 14, no. 7, pp. 911–913, Jul. 2002.

[2] T. Tanemura and K. Kikuchi, "Polarization-independent broad-band wavelength conversion using two-pump fiber optical parametric amplification without idler spectral broadening," *IEEE Photon. Technol. Lett.*, vol. 15, no. 8, pp. 1573–1575, Aug. 2003.

[3] S. Radic, C. J. McKinstrie, R. M. Jopson, J. C. Centanni, Q. Lin, and G. P. Agrawal, "Record performance of parametric amplifier constructed with highly nonlinear fiber," *Electron. Lett.*, vol. 39, pp. 838–839, 2003.

[4] S. Radic, C. Mckinstrie, R. Jopson, C. Jorgensen, K. Brar, and C. Headley, "Polarization dependent parametric gain in amplifiers with orthogonally multiplexed optical pumps," *Proc. OFC03*, vol. 2, pp. 508–510, 2003.

[5] Q. Lin and G. P. Agrawal, "Vector theory of four-wave mixing: Polarization effects in fiber-optic parametric amplifiers," *J. Opt. Soc. Amer. B, Opt. Phys.*, vol. 21, pp. 1216–1224, 2004.

[6] C. J. McKinstrie, S. Radic, and C. Xie, "Phase conjugation driven by orthogonal pum pwaves in birefringent fibers," *J. Opt. Soc. Amer. B, Opt. Phys.*, vol. 20, pp. 1437–1446, 2003.

[7] R. H. Stolen, J. P. Gordon, W. J. Tomlinson, and H. A. Haus, "Raman response function of silica-core fibers," *J. Opt. Soc. Amer. B, Opt. Phys.*, vol. 6, p. 1159, 1989.

[8] E. A. Golovchenko and A. N. Pilipetskii, "Unified analysis of four-photon mixing, modulational instability, and stimulated Raman scattering under various polarization conditions in fibers," *J. Opt. Soc. Amer. B, Opt. Phys.*, vol. 11, pp. 92–101, 1994.

[9] D. J. Dougherty, F. X. Karnter, H. A. Haus, and E. P. Ippen, "Measurement of the Raman gain spectrum of optical fibers," *Opt. Lett.*, vol. 20, pp. 31–33, 1995.

[10] G. P. Agrawal, *Nonlinear Fiber Optics*, 3rd ed. Boston, MA: Academic, 2001.

[11] D. Mahgerefteh, D. L. Butler, J. Goldhar, B. Rosenberg, and G. L. Burdge, "Technique for measurement of the Raman gain coefficient in optical fibers," *Opt. Lett.*, vol. 21, pp. 2026–2028, 1996.

[12] F. Vanholsbeeck, P. Emplit, and S. Coen, "Complete experimental characterization of the influence of parametric four-wave mixing on stimulated Raman gain," *Opt. Lett.*, vol. 28, pp. 1960–1962, 2003.